THE ASTROPHYSICAL JOURNAL, 410:567–573, 1993 June 20

THE IONIZING RADIATION OF SEYFERT 2 GALACTIC NUCLEI

LUIS C. HO
Department of Astronomy, University of California, Berkeley, CA 94720
JOSEPH C. SHIELDS
Department of Astronomy, The Ohio State University, 174 West 18th Avenue, Columbus, OH 43210
AND
ALEXEI V. FILIPPENKO[1]
Department of Astronomy, University of California, Berkeley, CA 94720
Received 1992 July 31; accepted 1992 December 14

ABSTRACT

We report the discovery of a nonrandom trend in the dispersion of emission-line intensity ratios for Seyfert 2 galaxies. The sense of this pattern suggests the influence of a single physical parameter, the hardness of the ionizing continuum (the ratio of X-ray to extreme ultraviolet fluxes), which controls the heating energy per ionizing photon. We compare the observed line ratios with new photoionization calculations and find that the observed distributions can be reproduced if the ionizing continuum is parametrized by a power law, $f_\nu \propto \nu^\alpha$, with α ranging from -1 to -2.5. Our results also suggest an inverse correlation between luminosity and continuum hardness for Seyfert 2 nuclei; if true, this trend extends a similar pattern known in quasars and Seyfert 1 galaxies to active galactic nuclei of lower luminosity. Samples of Seyfert 2 nuclei with improved selection uniformity are desirable for elaboration of these findings.

Subject headings: galaxies: abundances — galaxies: active — galaxies: nuclei — galaxies: Seyfert

1. INTRODUCTION

The optical properties of classical Seyfert 2 nuclei are characterized by the presence of (1) a bright, starlike nucleus and (2) narrow permitted and forbidden emission lines spanning a wide range of ionization stages. The broad (full width at half-maximum [FWHM] $\approx 10^3$–10^4 km s^{-1}) permitted lines present in Seyfert 1 galaxies are either very weak or absent in Seyfert 2 galaxies; the median FWHM of the lines is typically $\sim$450 km s^{-1} (Whittle 1992). In general, [O III] λ5007/H$\beta \gtrsim 3$ (Shuder & Osterbrock 1981), which implies that the level of excitation of the gas is high. At the same time, lines of low ionization can be fairly strong, indicative of ionization by a hard continuum with plenty of high-energy photons. These two properties broadly separate Seyfert 2 nuclei as a class from low-ionization nuclear emission-line regions (LINERs; Heckman 1980) and nuclei dominated by young stars (H II galaxies and starbursts) in optical and near-infrared line ratio diagnostic diagrams (Baldwin, Phillips, & Terlevich 1981; Veilleux & Osterbrock 1987, hereafter VO; Osterbrock, Tran, & Veilleux 1992).

The ionizing continuum of Seyfert 2 nuclei is generally assumed to be nonstellar in origin, due to the observed range of emission-line ionization state in these objects and their detection in some instances as significant X-ray sources. The ionizing spectral energy distribution at unobservable wavelengths can be estimated by extrapolation from longer wavelengths and independently constrained from emission-line measurements. Koski (1978) found that the optical continua of Seyfert 2 nuclei could be approximated by a stellar contribution diluted by a featureless continuum, with the latter component described by a power law with spectral index $\alpha = -1.5 \pm 0.5$ ($f_\nu \propto \nu^\alpha$). Koski estimated that the flux of the power-law component extrapolated to ionizing energies was sufficient for generating observed recombination line strengths. More recent observations with the *International Ultraviolet Explorer* at wavelengths closer to the Lyman limit, however, have challenged the latter conclusion in a number of cases (Neugebauer et al. 1980; Kinney et al. 1991). The apparent deficit of ionizing photons in these objects could be removed if the continuum spectral energy distribution features a strong local peak at extreme-ultraviolet (EUV) energies, or if the emission-line gas sees a stronger continuum than is observed along our line of sight—that is, if the continuum emission is anisotropic. Independent evidence for anisotropy in Seyfert 2 galaxies is provided by detection of Seyfert 1 emission scattered into our line of sight in a number of cases (e.g., Antonucci & Miller 1985), indicative of the presence of a broad-line region hidden from our direct view.

Extrapolation of the ionizing spectral energy distribution from direct continuum measurements of Seyfert 2 nuclei thus may not yield an accurate estimate of the radiation field incident on the emission-line clouds in these objects. If Seyfert 2 and Seyfert 1 nuclei are a common phenomenon mediated by orientation effects, a more reliable representation of Seyfert 2 continua may be simply the same spectral extrapolation applied to Seyfert 1 objects. Support for this approach is provided by the similarity in ultraviolet continuum slopes for the two classes ($\alpha \approx -1.3$; Kinney et al. 1991), and substantial overlap in luminosity distributions of penetrating hard X-rays for Seyfert 1 and 2 galaxies (Mulchaey, Mushotzky, & Weaver 1992). Assignment of such a simple correspondence between the two classes may be naive and misleading, however, since the geometric structure that determines the appearance of a Seyfert nucleus may itself be a function of intrinsic parameters that could include characteristics of the ionizing spectral energy distribution.

Given the uncertain details of Seyfert 2 continua, most photoionization calculations applied to these objects have represented the ionizing spectral energy distribution by a power

[1] Presidential Young Investigator.

law, which yields reasonable consistency between predicted and observed emission-line strengths (e.g., Koski 1978; Halpern & Steiner 1983; Ferland & Netzer 1983; Stasińska 1984a, b; Terlevich & Melnick 1985; Ferland & Osterbrock 1986, hereafter FO). Typical best-fit parameters for these calculations include (1) $\alpha = -1.5$, (2) ionization parameter (the ratio of ionizing photon density to nucleon density at the face of a cloud) $U = 10^{-2}$ to $10^{-2.5}$, (3) hydrogen density $n \approx 10^3$ cm^{-3}, and (4) abundances 1/3–1 × solar. Higher abundances may be tolerated when the emission-line region is treated as a multizonal system (e.g., Péquignot 1984); in fact, they may be necessary in many instances if contaminating circumnuclear emission is taken into account in the AGN measurements (Storchi-Bergmann 1991).

Despite the general acceptance of these simple models, it is clear that they succeed in reproducing the spectral features of Seyfert 2 galaxies as a class only in a very broad sense. For example, as the diagnostic diagrams of VO clearly show, there is considerable scatter around the theoretical predictions for Seyfert 2 galaxies. As VO point out, such a large scatter is unlikely to be caused entirely by observational error; rather, it probably reflects the simplicity of the assumptions of the models. Previous studies which sought to explain the average spectral properties of Seyfert 2 galaxies (e.g., FO) naturally do not account for all the objects in detail.

In this paper we show that much of the dispersion in the VO diagrams occurs in a preferred sense that suggests the influence of a single underlying physical parameter. The sense of this dispersion can be described as a correlation between the strengths of different optical forbidden lines relative to hydrogen recombination emission. This pattern suggests that the dispersion arises from variations in the average heating energy per ionization, and hence the hardness of the photoionizing continuum (i.e., the ratio of X-ray to EUV fluxes). We support this interpretation in detail with new photoionization calculations. We also report a possible inverse correlation between luminosity and continuum hardness in Seyfert 2 galaxies. The data are presented in § 2. Section 3 describes the photoionization calculations. Some implications of these results are discussed in § 4, and the main conclusions are summarized in § 5.

2. LINE RATIO DIAGRAMS

We present the data for Seyfert 2 galaxies in three diagnostic diagrams (Fig. 1) adapted from VO. The advantage of these diagrams (over most of those given by Baldwin et al. 1981) is that the emission-line intensity ratios involve lines closely separated in wavelength, minimizing uncertainties introduced in relative flux calibration and reddening correction. The data were selected from several sources. For classical Seyfert 2 galaxies and narrow-line radio galaxies (NLRGs; the narrow lines are thought to be nearly indistinguishable from those of Seyfert 2 galaxies), we chose the objects studied by Koski (1978), VO, and Osterbrock et al. (1992). In addition, we included the sample of "high-excitation galaxies" analyzed by Phillips, Charles, & Baldwin (1983; herafter PCB), which the authors concluded were very similar to Seyfert 2 galaxies. We did not include Mrk 298, Mrk 378, Mrk 507, Mrk 700, and NGC 6764 from Koski's sample; Ferland & Netzer (1983) classified Mrk 298, Mrk 700, and NGC 6764 as LINERs, but recent studies suggest that they may be nuclei dominated by relatively metal-rich H II regions with exceptionally low U (Filippenko & Terlevich 1992; Ho & Filippenko 1993; Ho, Filippenko, & Sargent 1993). Based on its location in the VO diagrams, we suspect that Mrk 378 also falls in the same category. Mrk 507, on the other hand, is probably a narrow-line Seyfert 1 galaxy (Halpern & Oke 1987). In constructing the subsequent line ratios, we adopted the reddening correction quoted by the respective authors.

Emission-line ratios plotted in Figure 1 show substantial scatter, yet there is a strong suggestion that the points in these diagrams are not distributed randomly. Specifically, there appears to be a preferred sense to the dispersion in each case, such that the measurements in each plot tend to populate a band with positive slope. We can quantitatively assess this trend with the Spearman rank-order test, which yields a probability P of consistency with the null hypothesis (no correlation between abscissa and ordinate; see Press et al. 1986). The results support the visual impression of nonrandom behavior, with $P = 4.8 \times 10^{-5}$ for log ([O I] λ6300/Hα) versus log ([O III] λ5007/Hβ) (Fig. 1*a*), $P = 7.8 \times 10^{-5}$ for log ([S II] λ6725/Hα) versus log ([O III] λ5007/Hβ) (Fig. 1*b*), and $P = 3.7 \times 10^{-3}$ for log ([N II] λ6583/Hα) versus log ([O III] λ5007/Hβ) (Fig. 1*c*).

The monotonic trend seen in the line ratio diagrams suggests the influence of a single underlying physical parameter describing the emission-line clouds, although the degree to which this parameter *dominates* the dispersion in Seyfert 2 emission-line ratios remains uncertain due to possible selection effects in the present sample. Heterogeneous selection criteria were used to identify the Seyfert 2 nuclei employed by VO and again here, so that selection effects in the data are likely to be complex. Delineation of a diagonal band in the line ratio diagrams is clearly strengthened by inclusion of the PCB objects (open boxes in Fig. 1), which may explain why the trends discussed here were not noted by VO, since VO did not include these sources in their study. The objects studied by PCB were previously identified by Sandage (1978) as high-excitation galaxies based on the strength of [O III] λ5007 relative to Hβ. While this selection might be expected to contribute primarily objects with relatively high values of [O III]/Hβ, Figure 1 illustrates that values of this ratio for the PCB galaxies actually show significant overlap with the observed distribution of points for the VO sample. This result may simply reflect the fact that, by definition, Seyfert 2 nuclei are "high-excitation"; indeed, PCB concluded that their sample members exhibited line ratios that closely resemble those of Seyfert 2 galaxies. Moreover, selection of objects based solely on the ordinate of Figure 1 does not provide an obvious means of populating a diagonal band in two dimensions for all three diagrams.

Selection effects influencing the distributions seen in Figure 1 can also be related, of course, to objects with ratios that are excluded from the plotted loci of points. In other words, the apparent correlation could be partially caused by systematic exclusion of existing objects with ratios falling to the lower right and upper left of the plotted distributions. One effect that will clearly act in this sense is related to our classification criteria, which distinguish Seyfert 2 nuclei from LINERs. In all three line ratio diagrams, LINERs populate a region below and slightly to the right of the Seyfert 2 locus, and the distinction between these classes could thus play a role in defining the nonrandom distribution for the latter category. Nonetheless, the preferred sense of dispersion is unlikely to be fully explained by this effect. At the highest line ratios, the Seyfert 2 line ratios appear to be increasingly decoupled from the observed LINER distribution (see also VO). A deficit of sources to the upper left of the Seyfert 2 loci additionally remains unexplained.

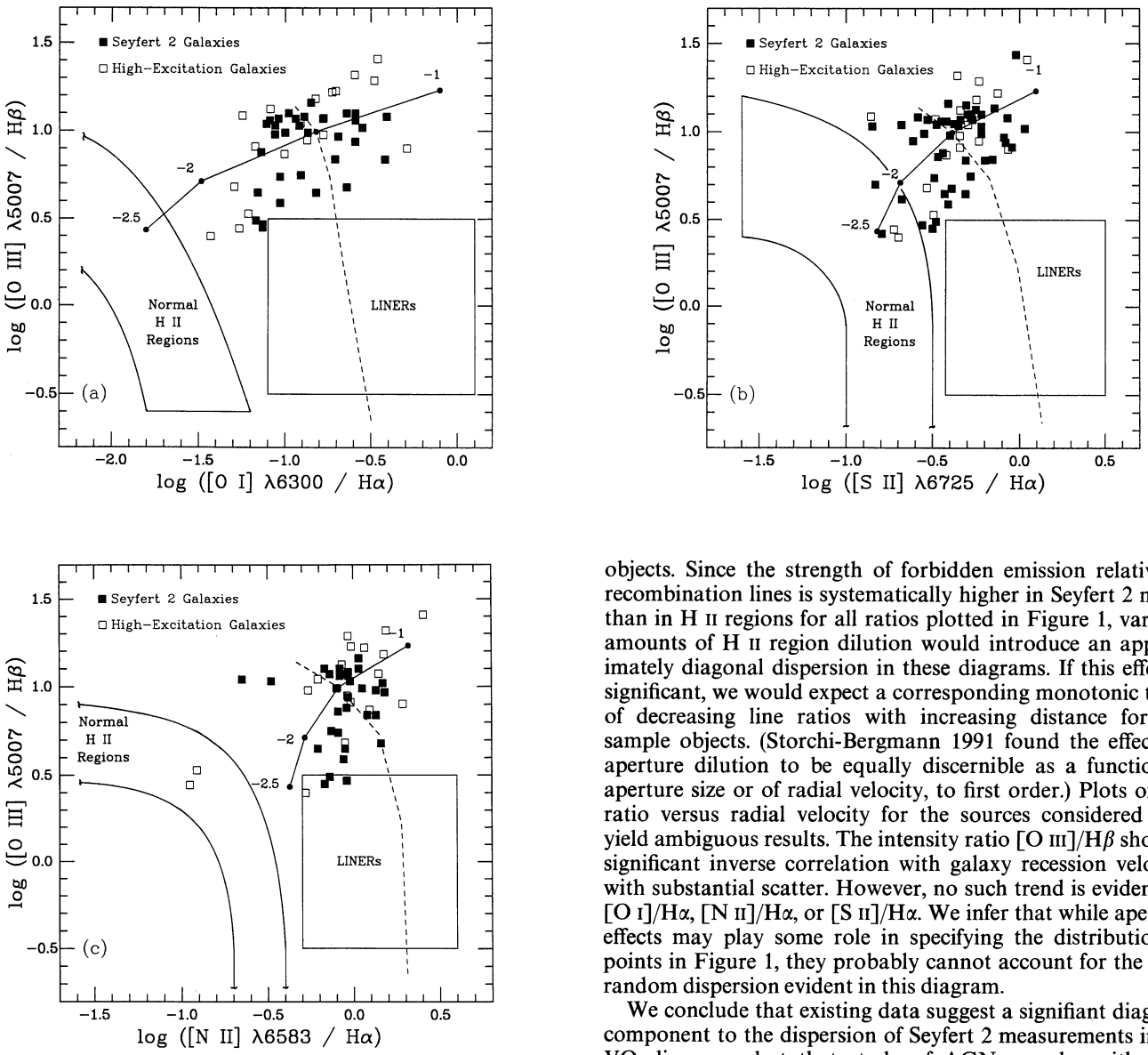

FIG. 1.—(*a*) VO diagram in which the line intensity ratio [O III] λ5007/Hβ is plotted against [O I] λ6300/Hα for different types of emission-line galaxies. The boxed regions indicate typical loci of normal H II regions and LINERs. Solid squares represent Seyfert 2 galaxies and NLRGs; open squares show the sample of "high-excitation galaxies" of PCB. Results of power-law photoionization models for $\alpha = -2.5$, -2, -1.5, and -1 are connected by the *solid* line. $U = 10^{-2.5}$ and $n = 10^{2.5}$ cm^{-3} are assumed. The results of varying U for a fixed $\alpha = -1.5$ are indicated by a *dashed* line for log $U = -2$, -2.5, -3, -3.5, and -4 (top to bottom). See text for details. (*b*) Line intensity ratios [O III] λ5007/Hβ plotted against [S II] λ6725/Hα. Symbols are the same as in Fig. 1*a*. (*c*) Line intensity ratios [O III] λ5007/Hβ plotted against [N II] λ6583/Hα. Symbols are the same as in Fig. 1*a*.

Aperture effects could also be responsible, in principle, for the diagonal trend seen in the VO diagrams. Storchi-Bergmann (1991) has noted that [N II]/Hα ratios taken from the literature for a large number of Seyfert 2 galaxies and LINERs tend to decrease with source distance. This trend probably reflects increasing dilution of the AGN spectrum by low-excitation (presumably H II region) circumnuclear emission included in the larger metric apertures of more distant objects. Since the strength of forbidden emission relative to recombination lines is systematically higher in Seyfert 2 nuclei than in H II regions for all ratios plotted in Figure 1, variable amounts of H II region dilution would introduce an approximately diagonal dispersion in these diagrams. If this effect is significant, we would expect a corresponding monotonic trend of decreasing line ratios with increasing distance for our sample objects. (Storchi-Bergmann 1991 found the effects of aperture dilution to be equally discernible as a function of aperture size or of radial velocity, to first order.) Plots of line ratio versus radial velocity for the sources considered here yield ambiguous results. The intensity ratio [O III]/Hβ shows a significant inverse correlation with galaxy recession velocity, with substantial scatter. However, no such trend is evident for [O I]/Hα, [N II]/Hα, or [S II]/Hα. We infer that while aperture effects may play some role in specifying the distribution of points in Figure 1, they probably cannot account for the non-random dispersion evident in this diagram.

We conclude that existing data suggest a signifiant diagonal component to the dispersion of Seyfert 2 measurements in the VO diagrams, but that study of AGN samples with well-defined selection criteria and aperture dimensions is necessary in order to delineate the details of line ratio loci. In the absence of obvious selection effects responsible for the trend seen in the existing data, we have examined whether this dispersion can be reproduced by an underlying physical parameter describing the emission-line regions.

3. RESULTS OF PHOTOIONIZATION MODELS

To our knowledge, the origin of the distinctive dispersion in the line ratio diagrams for Seyfert 2 nuclei has not been explicitly identified in published photoionization calculations. We consequently generated new theoretical photoionization calculations using the code CLOUDY (Ferland 1991) in an effort to match the observed correlations presented in the previous section. The code solves the equations of statistical and thermal equilibrium, and produces a self-consistent model of the run of temperature and ionization as a function of depth into the cloud. For simplicity, we assumed a constant density cloud with plane-parallel geometry. A sequence of models was

calculated in which α was set to 0, -0.5, -1, -1.5, -2, and -2.5 in the spectral range between 10 μm and 50 keV. The low-energy cutoff has a slope of $\alpha = 2.5$, appropriate for a self-absorbed synchrotron continuum. The constraint that the energy output of AGNs does not exceed the observed 60–400 keV diffuse background has led Rothschild et al. (1983) to suggest that there is a break in the continuum above 50 keV with a slope of -1.67. We assume that at high energies the slope is $\alpha = -2$. For each value of α, we varied log U from -2 to -3, a range which encompasses values previously determined by other workers. In order to examine the effects of variation in density, we chose values for the total hydrogen density ranging from log $(n/\mathrm{cm}^{-3}) = 2.5$ to 5. The calculations were stopped when the temperature fell to 4000 K, below which it was verified that little optical emission is expected. Our calculations assume solar abundances for all the elements (Grevesse & Anders 1989), with the exception of nitrogen, for which we assumed a selective enhancement by a factor of 2 above solar as suggested by previous analyses (Storchi-Bergmann 1991, and references therein). The gas was assumed to be dust-free.

While the observed trends in Seyfert 2 line ratios can be described to some degree as correlated levels of excitation for the different forbidden species, sequences of variable U do not account for this pattern. In fact, the dispersion runs orthogonal to the sense predicted by variations in U, as can be seen by the dashed line in Figures 1*a*–1*c* depicting the results of varying U (10^{-2} to 10^{-4}) while $\alpha = -1.5$ and log $(n/\mathrm{cm}^{-3}) = 2.5$ remain fixed (see also VO Figs. 4–6). Differences in U are, in fact, thought to be the basis for observed distinctions between the emission-line spectra of Seyfert 2 nuclei and photoionized LINERs (Ferland & Netzer 1983; Halpern & Steiner 1983), although modest variations in U may well be responsible for much of the vertical spread of Seyfert 2 points in Figure 1.

Forbidden emission-line strengths are sensitive to cloud density, but variations in this parameter also do not satisfactorily explain the diagonal dispersions in Figure 1. For forbidden lines with high critical densities, increases in density through a low range can lead to enhancements of these lines as they take on the cooling function of other transitions that become collisionally suppressed. The magnitude of this effect is not sufficient to account for the observed spread in values, and the [S II] $\lambda\lambda$6716, 6731 lines additionally become weaker relative to Hα rather than stronger at densities exceeding the relatively low critical density ($\sim 10^3$ cm^{-3}) of these features. Variations in density may account for a significant fraction of the observed scatter in Seyfert 2 line ratios, but appear unable to explain the correlations present in these ratios.

Variations in continuum hardness provide a more likely source of the nonrandom dispersion in line ratios. The strength of forbidden emission reflects the average energy of collisional electrons, which in turn responds to the average energy per ionizing photon. The preferred direction of scatter in the two-dimensional VO diagrams is qualitatively consistent in all cases with variations in hardness of the ionizing continuum. This trend is evident quantitatively in the grid of nebular models calculated by Stasińska (1984a), although she focuses in her analysis on line ratio plots that differ from the VO diagrams employed here (Stasińska 1984b).

The best-fitting model resulting from the present calculations is plotted in Figure 1 as a solid line. The points shown are for $\alpha = -1$, -1.5, -2, and -2.5, log $U = -2.5$, and log $(n/\mathrm{cm}^{-3}) = 2.5$. This model quite successfully reproduces the horizontal dispersion seen in the VO diagrams. The vertical dispersion (i.e., the range of values for [O III] λ5007/Hβ) can be interpreted as the existence of a range in U (10^{-2} to 10^{-3}) and n ($10^{2.5}$–10^5 cm^{-3}). By adjusting suitable combinations of U and n, the dispersion in the vertical direction can be easily reproduced, with minor modifications to the range of α. The predicted line intensity ratios are given in Table 1. Column (1) lists the line identifications. Column (2) shows the composite spectrum for Seyfert 2 galaxies, adapted from FO. Columns (3)–(6) list the predicted $F(\lambda)/F(\mathrm{H}\beta)$ ratio for our best-fitting models with $\alpha = -1$, -1.5, -2, and -2.5, respectively. While variation in continuum hardness offers an attractive explanation for the nonrandom dispersion in the line ratio diagrams, we do not claim that this represents a unique interpretation of the data. In particular, variation in any significant source of nebular heating (e.g., cosmic rays) would be expected to promote a qualitatively similar dispersion.

A close examination of the figures shown in VO indicates that LINERs also exhibit a very large dispersion in their low-ionization line ratios, although a comparable scatter is also apparent in [O III] λ5007/Hβ. Recent photoionization calculations (Ho et al. 1993) suggest that the spread of the observed line ratios of LINERs may best be explained by variations in both the density and the spectral index of the power-law ionizing continuum. Those LINERs with weak low-ionization lines, which contribute substantially to the apparent scatter among the observed line ratios, may be unrelated to the AGN phenomenon and may instead be powered by a thermal ionizing continuum from hot O-type stars (Filippenko & Terlevich 1992; Ho et al. 1993). Alternatively, Shields (1992) suggests that the spectral features of most LINERs are consistent with photoionization by O-stars in which a range of gas densities and ionization parameters characterize the circumstellar media.

4. DISCUSSION

4.1. *Assumptions of the Models*

Our main result suggests that the primary parameter responsible for the observed dispersion seen in the optical line ratios is the hardness of the ionizing continuum. If the shape of the ionizing continuum is assumed to be a power law, its variation in hardness (basically the ratio of X-ray to EUV fluxes, since only these high-energy photons affect the ionization structure of the gas) can be conveniently represented by a variation in the spectral index, α. Other parameters such as the ionization parameter, density, abundances, and grains change the line ratios in various ways, but do not appear to be dominant in reproducing the observed trends. The values of α which bracket the observed line ratios range from -1 to -2.5.

Although we have adopted the simple representation of a power law for the ionizing continuum in our calculations, we do not imply that such a representation necessarily reflects the "true" nature of the ionizing continuum. Measurements of a handful of bright QSOs and Seyfert 1 galaxies indicate that their continua can be decomposed into several basic components. The ultraviolet through X-ray continuum of powerful AGNs is typically represented by a broad excess of UV emission (the "big blue bump"; e.g., Malkan & Sargent 1982) that declines at UV or EUV energies, meeting an X-ray power law with typical $\alpha \approx -0.7$ (e.g., Elvis & Lawrence 1985). The detailed spectral energy distribution is poorly determined through the EUV region. However, previous photoionization

TABLE 1

PREDICTED LINE INTENSITY RATIOS[a]

Line (1)	Mean[b] (2)	$\alpha = -1$ (3)	-1.5 (4)	-2 (5)	-2.5 (6)
Lyα λ1216	55 $\pm$ 20	28.17	25.46	25.04	24.87
Si IV λ1397	...	0.055	0.0055	0.0004	...
C IV λ1549	12 $\pm$ 8	0.42	0.035	0.003	0.0002
Si III λ1895	...	0.26	0.08	0.02	0.006
C III] λ1909	5.5 $\pm$ 3.7	0.64	0.13	0.03	0.009
C II] λ2326	...	0.92	0.22	0.09	0.05
Si II λ2336	...	0.21	0.06	0.03	0.01
Mg II λ2798	1.8 $\pm$ 1.5	3.04	0.97	0.46	0.26
[Ne V] λ3426	1.2 $\pm$ 0.2	0.12	0.012	0.0008	...
[O II] λ3727	3.2 $\pm$ 1.7	5.32	2.55	1.59	1.10
[Ne III] λ3869	1.4 $\pm$ 0.4	1.91	0.86	0.41	0.21
[Fe V] λ3892	$<$0.1	0.19	0.08	0.02	0.005
[S II] λ4072	0.30 $\pm$ 0.2	0.14	0.05	0.02	0.02
[O III] λ4363	0.21 $\pm$ 0.1	0.15	0.04	0.01	0.003
He II λ4686	0.29 $\pm$ 0.1	0.19	0.12	0.07	0.04
Hβ λ4861	1.00	1.00	1.00	1.00	1.00
[O III] λ5007	10.8 $\pm$ 3.0	17.02	9.92	5.16	2.71
[Fe VI] λ5177	$<$0.1	0.036	0.009	0.001	0.0005
[N I] λ5200	0.15 $\pm$ 0.09	0.72	0.13	0.02	0.01
He I λ5876	0.13 $\pm$ 0.06	0.11	0.12	0.13	0.14
[Fe VII] λ6087	0.10 $\pm$ 0.05	0.046	0.006	0.0004	...
[O I] λ6300	0.57 $\pm$ 0.2	2.18	0.41	0.09	0.04
[Fe X] λ6375	0.04 $\pm$ 0.04	0.0002	...	...	...
Hα λ6563	3.1 $\pm$ 0.1	2.76	2.71	2.69	2.68
[N II] λ6583	2.9 $\pm$ 1.0	5.75	2.22	1.39	1.13
[S II] λ6725	1.5 $\pm$ 0.5	3.44	1.11	0.55	0.40
[Ar III] λ7136	0.24 $\pm$ 0.07	0.27	0.19	0.14	0.09
[O II] λ7325	...	0.11	0.05	0.02	0.01
[S III] λ9069	...	1.09	0.73	0.51	0.38
[S III] λ9532	...	2.83	1.90	1.33	0.99
[Ne III] 15.6 μm	...	4.16	2.76	2.26	1.98

[a] Power-law ionizing continuum models assuming log $U = -2.5$, log $(n/\mathrm{cm}^{-3}) = 2.5$, and solar abundances (except N, which is 2 times solar).

[b] Composite spectrum of Seyfert 2 galaxies taken from Ferland & Osterbrock 1986.

calculations suggest that AGN emission-line behavior is sensitive to the broad-band ionizing continuum properties, but relatively insensitive to fine details of the EUV/X-ray spectral energy distribution (e.g., Binette, Robinson, & Courvoisier 1988). The results presented here for power-law continua can thus be generalized for more complicated continuum shapes, with continuum hardness referring to the average energy per ionizing photon.

The calculations described here assume a single population of clouds in terms of n and U, which almost certainly represents an oversimplification of Seyfert 2 nebulae. Recent studies have amassed evidence that a range of densities ($n \approx 10^2$–10^7 cm^{-3}) exists in the narrow-line region (NLR) (Pelat, Alloin, & Fosbury 1981; Filippenko & Halpern 1984; Filippenko 1985; De Robertis & Osterbrock 1986). Inclusion of multiple nebular components changes the predicted line ratios in various ways and can lead to improved agreement with the average Seyfert 2 spectrum (e.g., Stasińska 1984b; Binette et al. 1988; FO). We have chosen to adopt the assumption of a single density for the sake of simplicity and in order to minimize the number of free parameters. Comparison of our line predictions for the $\alpha = -1.5$ calculation (col. [4] of Table 1) with the results of the multizonal model of FO indicates that the agreement is reasonably close for most of the lines. While object-to-object variations in nebular structure will introduce scatter in the line ratio diagrams, we know of no obvious structural parameter that, when varied, will lead to a preferentially diagonal dispersion in the VO diagrams. The physical origin suggested previously, ionizing continuum hardness, will influence the average photoelectron energy and nebular heating regardless of the detailed structure of a cloud ensemble.

4.2. *Luminosity-Continuum Hardness Correlation*

Much evidence has been accumulated to suggest that, among quasars and Seyfert 1 galaxies, there is an inverse correlation between the luminosity of an object and the hardness of its optical to X-ray continuum (Kriss 1988; Mushotzky & Wandel 1989). This observational trend is usually interpreted as implying that more luminous objects have larger big blue bumps. The extent to which this trend continues to lower luminosities is not well known. Recent evidence suggests that the same phenomenon persists to a few well-studied LINERs (Mushotzky 1993). The results of our work may shed some light on the situation for Seyfert 2 galaxies, which remains uncertain. If all Seyfert 2 galaxies are in fact obscured Seyfert 1 galaxies, then any measurements of the continuum luminosity and of the hardness of the ionizing continuum, such as by determining the optical to X-ray slope of the continuum, would be heavily affected by the presence of an obscuring torus. The torus would be optically thick to optical, UV, and soft X-ray radiation, but not to hard X-rays in most cases. X-ray studies of a number of Seyfert 2 galaxies suggest the presence of very large column densities, most likely originating from an obscuring torus (Awaki et al. 1991; Mulchaey et al. 1992). Direct estimation of ionizing continuum hardness as a function of luminosity in Seyfert 2 galaxies is thus problematic.

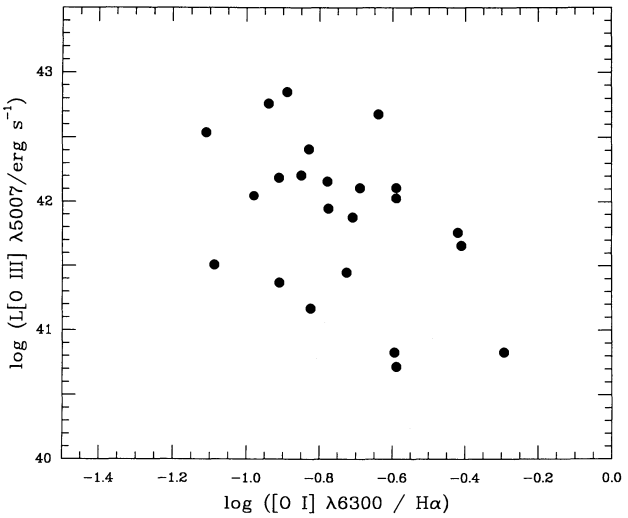

FIG. 2.—Log (L[O III] λ5007) is plotted against log ([O I] λ6300/Hα) for all galaxies in our sample that have reliable measurements of the luminosity of [O III] λ5007 (in units of ergs s^{-1}).

Among those Seyfert 2 galaxies for which there are reliable meaurements of the luminosity of [O III] λ5007, L([O III]), we find that there may be an inverse correlation between L([O III]) and the relative strength of the low-ionization lines, most notably for [O I] λ6300 (Fig. 2), although the case is marginal with the present data set. The Spearman rank-order test yields $P = 3.2 \times 10^{-2}$. If one assumes that an inverse correlation does exist between the luminosity of Seyfert 2 galaxies and the hardness of their ionizing continua, then the sense of this correlation is easily understood. An object with lower luminosity has a harder ionizing spectrum, which in turn generates a larger partly ionized zone in the line-emitting clouds where most of the [O I] emission is produced.

If this result is true, the luminosity-continuum hardness correlation, previously known for high-luminosity AGNs, may also extend to AGNs of lower luminosity such as Seyfert 2 galaxies. The influence of the luminosity-continuum hardness correlation on emission-line strengths has previously been identified in a principal-components analysis of quasar spectra by Boroson & Green (1992). However, this is the first time to our knowledge that a manifestation of this trend is suggested in the emission lines of Seyfert 2 galaxies. Since our determination of the hardness of the continuum is based on photoionization modeling and not from direct measurements, our results are not affected by possible obscuration from a torus. Furthermore, the luminosities shown in Figure 2 originate directly from the NLR, which presumably has a nearly unobstructed view of the nucleus regardless of the galaxy's orientation relative to the observer. Because of the small size and nonuniform selection criteria of the present sample, we emphasize that a complete data set extending over a larger range of luminosity is needed to confirm this result.

Finally, as a cautionary note, we observe that plots of luminosity versus line ratio map in a rough sense to distance versus line ratio, such that correlations like the one suggested in Figure 2 are again susceptible to aperture dilution effects (§ 2). As noted previously, no correlation is evident in the present sample between distance and [O I]/Hα, so that any trend present in Figure 2 may well be genuine. Interestingly, no correlation is seen between L([O III]) and [O III]/Hβ, despite the existence of an inverse relation between galaxy velocity and [O III]/Hβ (§ 2). Nonetheless, future studies directed at studying line ratios as a function of source luminosity would profit from careful control of metric aperture dimensions.

5. CONCLUSIONS

We identify an apparently nonrandom dispersion of the low-ionization line ratios among Seyfert 2 nuclei in the three optical emission-line ratio diagnostic diagrams of VO. The sense of this dispersion can be described by a correlation between the [O I]/Hα, [O III]/Hβ, [N II]/Hα, and [S II]/Hα intensity ratios. We are unable to identify any selection or experimental effects that can account for this pattern, although Seyfert 2 samples with homogeneous selection criteria are desirable for determining the extent to which the dispersion of line ratios is dominated by this trend. Comparison of the data with existing and new photoionization calculations implies that the preferential sense of the observed dispersion cannot be explained by simple variations in ionization parameter, density, or abundances. However, the observational trend can be reproduced if one assumes that there exists a range in the hardness of the photoionizing continuum. When the ionizing spectral energy distribution is parameterized as a power law, we find that the observed line ratios are bracketed by variations of continuum spectral index spanning $\alpha = -1$ to -2.5. Additional scatter in the vertical direction of the VO diagrams may reflect intrinsic variation in the density, ionization parameter, or abundances in the line-emitting gas.

The present data tentatively suggest an inverse relationship between Seyfert 2 luminosity, as measured by [O III], and ionizing continuum hardness deduced from line intensity ratios. If real, this trend extends a correlation seen in Seyfert 1 nuclei, quasars, and possibly LINERs to the Seyfert 2 class.

We thank Jules Halpern for a critical reading of the manuscript and an anonymous referee for valuable comments. We acknowledge the financial support of NSF grant AST-8957063 and NASA grant NAG 5-1800 to A. V. F. The work of J. C. S. was financed by NSF grant AST-9019692 to G. J. Ferland, whom we thank for generously providing his CLOUDY code.

REFERENCES

Antonucci, R. R. J., & Miller, J. S. 1985, ApJ, 297, 621
Awaki, H., Koyama, K., Inoue, H., & Halpern, J. P. 1991, PASJ, 43, 195
Baldwin, J. A., Phillips, M. M., & Terlevich, R. 1981, PASP, 93, 5
Binette, L., Robinson, A., & Courvoisier, T.-L. 1988, A&A, 194, 65
Boroson, T. A., & Green, R. F. 1992, ApJS, 80, 109
De Robertis, M. M., & Osterbrock, D. E. 1986, ApJ, 301, 727
Elvis, M., & Lawerence, A. 1985, in Astrophysics of Active Galaxies and Quasi-Stellar Objects, ed. J. S. Miller (Mill Valley, CA: Univ. Science Books), 289
Ferland, G. J. 1991, Ohio State Univ. Internal Rep. 91-01 (Columbus: OSU Astronomy)
Ferland, G. J., & Netzer, H. 1983, ApJ, 264, 105
Ferland, G. J., & Osterbrock, D. E. 1986, ApJ, 300, 658 (FO)
Filippenko, A. V. 1985, ApJ, 289, 475
Filippenko, A. V., & Halpern, J. P. 1984, ApJ, 285, 458
Filippenko, A. V., & Terlevich, R. 1992, ApJ, 397, L79
Grevesse, N., & Anders, E. 1989, in AIP Conf. Proc. 183, Cosmic Abundances of Matter, ed. C. J. Waddington (New York: AIP), 1
Halpern, J. P., & Oke, J. B. 1987, ApJ, 312, 91
Halpern, J. P., & Steiner, J. E. 1983, ApJ, 269, L37
Heckman, T. M. 1980, A&A, 87, 152
Ho, L. C., & Filippenko, A. V. 1993, in The Nearest Active Galaxies, ed. J. Beckman, Ap&SS, in press
Ho, L. C., Filippenko, A. V., & Sargent, W. L. W. 1993, ApJ, in press

Kinney, A. L., Antonucci, R. R. J., Ward, M. J., Wilson, A. S., & Whittle, M. 1991, ApJ, 377, 100
Koski, A. T. 1978, ApJ, 223, 56
Kriss, G. A. 1988, ApJ, 324, 809
Malkan, M. A., & Sargent, W. L. W. 1982, ApJ, 254, 22
Mulchaey, J. S., Mushotzky, R. F., & Weaver, K. A. 1992, ApJ, 390, L69
Mushotzky, R. F. 1993, in The Nearest Active Galaxies, ed. J. Beckman (Madrid: CSIC), in press
Mushotzky, R. F., & Wandel, A. 1989, ApJ, 339, 674
Neugebauer, G., et al. 1980, ApJ, 238, 502
Osterbrock, D. E., Tran, H. D., & Veilleux, S. 1992, ApJ, 389, 196
Pelat, D., Alloin, D., & Fosbury, R. A. E. 1981, MNRAS, 195, 787
Péquignot, D. 1984, A&A, 131, 159
Phillips, M. M., Charles, P. A., & Baldwin, J. A. 1983, ApJ, 266, 485 (PCB)
Press, W. H., Flannery, B. P., Teukolsky, S. A., & Vetterling, W. T. 1986, Numerical Recipes, the Art of Scientific Computing (Cambridge: Cambridge Univ. Press)
Rothschild, R., Mushotzky, R. F., Baity, W., Gruber, D., Matteson, J., & Peterson, L. 1983, ApJ, 269, 423
Sandage, A. 1978, AJ, 83, 904
Shields, J. C. 1992, ApJ, 399, L27
Shuder, J. M., & Osterbrock, D. E. 1981, ApJ, 250, 55
Stasińska, G. 1984a, A&AS, 55, 15
———. 1984b, A&A, 135, 341
Storchi-Bergmann, T. 1991, MNRAS, 249, 404
Terlevich, R., & Melnick, J. 1985, MNRAS, 213, 841
Veilleux, S., & Osterbrock, D. E. 1987, ApJS, 63, 295 (VO)
Whittle, M. 1992, ApJ, 387, 109